Contract # F49620-92-J-0299

THE OHIO STATE UNIVERSITY

FINAL REPORT ON:

INTEGRATED CIRCUITS FOR DISTRIBUTED CONTROL-(AASERT FY91)

FOR 1992-95

Ü. Özgüner
The Ohio State University
1314 Kinnear Road
Columbus, Ohio 43212

January 1996

Final Report for Period September 1, 1992 - October 14, 1995

RF Project No. 769993/726322

REPORT DOCUMENTATION PAGE

Form Approved
OMB No. 0704-0188

1. AGENCY USE ONLY *(Leave blank)*	2. REPORT DATE	3. REPORT TYPE AND DATES COVERED
	~~05 Feb 96~~	Final Technical Report 15 Jun 92 to 14 Oct 95

4. TITLE AND SUBTITLE
INTEGRATED CIRCUITS FOR DISTRIBUTED CONTROL-(AASERT FY91)

5. FUNDING NUMBERS
F49620-92-J-0299

6. AUTHOR(S)
U. Ozguner

7. PERFORMING ORGANIZATION NAME(S) AND ADDRESS(ES)
The Ohio State University
1314 Kinnear Road
Columbus, OH 43212

8. PERFORMING ORGANIZATION REPORT NUMBER

9. SPONSORING/MONITORING AGENCY NAME(S) AND ADDRESS(ES)
AFOSR/NA
110 Duncan Ave, B 115
Bolling AFB, DC 20332-8050

10. SPONSORING/MONITORING AGENCY REPORT NUMBER
F49620-92-J-0299

11. SUPPLEMENTARY NOTES

12a. DISTRIBUTION AVAILABILITY STATEMENT
Approved for Public Release; Distribution Unlimited.

12b. DISTRIBUTION CODE

13. ABSTRACT *(Maximum 200 words)*

The central focus of the effort on this project has been the development of analog VLSI circuit models intended for use in distributed, model-based control of vibrations for flexible structures. The availability of piezo strain elements and memory alloys has created the possibility for actively controlled composite structures in which actuation is integrated with the structure. The advances in miniaturization of analog VLSI circuits allow analog models, controllers, and observers to be embedded directly on flexible structures with little increase in weight[1, 2, 3]. thus, a chip model of a substructure could be integrated directly into the controller and embedded in the substructure with the actuation. The research presented in this report has involved designing analog models of flexible structures for applications involving sophisticated embedded control applications.

14. SUBJECT TERMS

15. NUMBER OF PAGES
23

16. PRICE CODE

17. SECURITY CLASSIFICATION OF REPORT	18. SECURITY CLASSIFICATION OF THIS PAGE	19. SECURITY CLASSIFICATION OF ABSTRACT	20. LIMITATION OF ABSTRACT
UNCLASSIFIED	UNCLASSIFIED	UNCLASSIFIED	UL

Project Title: Integrated Circuits for Distributed Control–(AASERT FY91)

Grant Number: F49620-92-J-0299

Parent Award: F49620-89-C-0046 / F49620-92-J-0460

Parent Project Title: Analysis and Control of Interconnected Structures

Students Supported by Parent Project:
W.-C. Su, D. Clancy, L. Lenning (at different times)

Students Supported by this Project:
F. Green–graduated August 1993, A. Shah–graduated August 1994, L. Lenning–continuing

Publications on research for this project:

1. Ü. Özgüner and L. Lenning, "The intelligence between sensing and actuation in smart structures," in *Proceedings of the ADPA/AIAA/ASME/SPIE Conference on Active Materials and Adaptive Structures*, pp. 825-830, The Institute of Physics, 1992.

2. S. V. Drakunov, Ü. Özgüner, and L. Lenning, "Use of neural networks and sliding modes in vibration damping," in *Smart Structures and Materials 1993: Mathematics in Smart Structures* (H. T. Banks, ed.), pp. 174-181, Proc. SPIE 1919, 1993.

3. A. Shah, L. Lenning, S. Bibyk, and Ü. Özgüner, "Flexible beam modeling with analog VLSI circuits," in *Adaptive Structures and Composite Materials: Analysis and Application*, vol. AD-45/MD-54, pp. 261-265, ASME, 1994.

4. A. Shah, L. Lenning, Ü. Özgüner, and S. Bibyk, "Analog VLSI circuit models for smart flexible structures," in *Smart Structures and Materials 1995: Mathematics and Control in Smart Structures* (V. V. Varadan, ed.), Proc. SPIE 2442, 1995.

5. L. Lenning, A. Shah, Ü. Özgüner, and S. Bibyk, "Control of flexible structures using analog VLSI circuit models," submitted for publication.

ABSTRACT

In this report, we summarize the final results of the research performed at The Ohio State University on the AASERT Project F49620-92-J-0299 entitled **Integrated Circuits for Distributed Control-(AASERT FY91)**. This AASERT Project, which was initiated on 1 September 1992 and completed 14 October 1995, has been sponsored by the Air Force Office of Scientific Research (AFSC) and is linked to the Project F49620-92-J-0460 entitled *Analysis and Control of Interconnected Structures.*

The central focus of the effort on this project has been the development of analog VLSI circuit models intended for use in distributed, model-based control of vibrations for flexible structures. The availability of piezo strain elements and memory alloys has created the possibility for actively controlled composite structures in which actuation is integrated with the structure. The advances in miniaturization of analog VLSI circuits allow analog models, controllers, and observers to be embedded directly on flexible structures with little increase in weight [1, 2, 3]. Thus, a chip model of a substructure could be integrated directly into the controller and embedded in the substructure with the actuation. The research presented in this report has involved designing analog models of flexible structures for applications involving sophisticated embedded control applications.

Contents

1. INTRODUCTION

In this report, we summarize the final results of the research performed at The Ohio State University on the AASERT Project F49620-92-J-0299 entitled **Integrated Circuits for Distributed Control-(AASERT FY91)**. This AASERT Project, which was initiated on 1 September 1992 and completed 14 October 1995, has been sponsored by the Air Force Office of Scientific Research (AFSC) and is linked to the Project F49620-92-J-0460 entitled *Analysis and Control of Interconnected Structures.*

The central focus of the effort on this project has been the development of analog VLSI circuit models intended for use in distributed, model-based control of vibrations for flexible structures. The availability of piezo strain elements and memory alloys has created the possibility for actively controlled composite structures in which actuation is integrated with the structure. The advances in miniaturization of analog VLSI circuits allow analog models, controllers, and observers to be embedded directly on flexible structures with little increase in weight [1, 2, 3]. Thus, a chip model of a substructure could be integrated directly into the controller and embedded in the substructure with the actuation. The research presented in this report has involved designing analog models of flexible structures for applications involving sophisticated embedded control applications.

A smart structure requires an internal knowledge of self in order to act intelligently[1]. This knowledge may be acquired from local models of substructure dynamics. In systems/control terminology, the use of this knowledge to determine some intelligent action is model-based control.

A large class of interconnected structures–including most structures comprised of physical systems–have models represented by electrical networks. By actually building electrical network models of substructure building–blocks, the interconnection of the subnetworks will provide the same system response as the assembly of the mechanical substructures. Thus, VLSI circuit chips can be developed to represent portions of trusses, plates, appendages, etc., and an analog representation of the complete system such as an airplane wing or a space station can be assembled. Furthermore, these models may be used in any of the large class of control approaches which incorporate a nominal model of the system being controlled within the feedback control loop. With the development of these VLSI circuit models, compact, cost-effective integrated controllers may eventually become available for many applications.

Although finite element models (FEM) are well-suited for digital computation, the also have features which make them desirable for analog computation. The differential equations have a very repetitive structure and must be solved simultaneously in real time. Thus, the parallel architecture of the FEM is actually better suited for continuous-time analog signal processing than for implementation on a time-multiplexed DSP architecture. Another advantage of the analog solution is that all states of the system are available simultaneously and continuously in real time. The goal of the research presented here is to devise analog VLSI circuits which are easily connectable and represent finite elements of the FEM of a

flexible structure. These elemental circuits should be tunable such that resonant modes and effective damping ratios for each element may be adjusted. From these elemental circuits, an entire structure could be easily modeled in analog hardware which could provide real-time data for use in embedded controllers.

In this report, circuit-based modeling of structures is briefly summarized. A design methodology to convert a FEM into analog circuitry which can be fabricated on a VLSI chip is presented. A simple circuit prototype and test results for a VLSI chip are demonstrated. Control applications for such VLSI circuit models are developed and simulation results are presented for a simple example which illustrate the concept that such analogous VLSI circuits can directly aid in generating the feedback control for large structural systems.

2. MODELING OF FLEXIBLE STRUCTURES

2.1 Finite Element Modeling

The FEM for a flexible beam has been widely researched and is available in the literature [4, 5]. A FEM is generally of the form

$$M\ddot{q} + \beta\dot{q} + Kq = F_{ext} \tag{2.1}$$

where M is the mass matrix, K is the stiffness matrix, β is the damping matrix, F_{ext} is the vector of generalized forces, and q is the nodal displacement vector. This matrix equation can be rewritten in state-space form

$$\dot{x} = Ax + Bu \tag{2.2}$$

$$y = Cx + Du \tag{2.3}$$

where $x = [q\ \dot{q}]^T$, and

$$A = \begin{bmatrix} 0 & I \\ -M^{-1}K & -M^{-1}\beta \end{bmatrix} \qquad B = \begin{bmatrix} 0 \\ -M^{-1} \end{bmatrix}. \tag{2.4}$$

The state-space matrices for an FEM of a flexible structure generally are sparse, repetitive, and banded or block-diagonal. Thus, interconnecting the circuit equivalents of the structural elements requires relatively few connections. Generally, relatively few *unique* finite elements are used to model a flexible structure. Often, for instance, all elements are assumed to have the same size, shape, inertia, and stiffness properties. Thus, the FEM has a highly repetitive structure. The repetitive structure allows additional elements to be easily integrated into

the network–extending the order of the system. Also due to the repetitive structure, analog VLSI circuit equivalents of the FEM require very repetitive hardware. While the sparse and repetitive nature of the state space FEM formulation make finite element modeling particularly attractive for analog computation, non-sparse general state-space modeling is also possible using the same approach.

2.2 Circuit Analogies for Flexible Structure Modeling

Large flexible structures may be viewed as an interconnection of several substructures where the vibration control problem can be approached as a question of power transfer—similar to problems in transmission line theory or electrical circuits. Circuit analogies of mechanical systems have existed for many years. When the history of mechanical and electrical systems is considered, the complementary progress of the two areas is evident. Results of electrical network theory have many applications to acoustical, mechanical, and electromechanical systems. Included in these applications is vibration control of large flexible structures. Typical examples of circuit analogies for mechanical systems are shown in Table 2.2. Using

Table 2.1: Electrical / Mechanical System Analogies

Electrical	Mechanical (Linear)	Mechanical (Rotational)
voltage, V	velocity, v, $\dot{x}$	angular velocity, ω, θ
current, I, $\dot{q}$	force, F	torque, τ
charge, q	momentum, P	angular momentum, h
flux linkage, λ	displacement, x	angular displacement, θ
capacitance, C	mass, M	moment of inertia, J
inverse inductance, $\frac{1}{L}$	stiffness, K	rotational stiffness, K
inverse resistance, $\frac{1}{R}$	damping, β	damping, β

these variable and element analogies, the equations for electrical and mechanical systems are:

$$I_{ext} = C\dot{V} + \frac{1}{R}V + \frac{1}{L}\int V\,dt \tag{2.5}$$

$$F_{ext} = M\ddot{x} + \beta\dot{x} + Kx \tag{2.6}$$

$$\tau_{ext} = J\ddot{\theta} + \beta\dot{\theta} + K\theta \tag{2.7}$$

Connecting substructures is analogous to connecting circuit subnetworks. The impedance of the entire structure can be determined from the impedances of the interconnected substructures as one would determine the impedance of a circuit.

3. CIRCUIT EQUIVALENT OF A MASS-SPRING SYSTEM

The simplest type of flexible structure is a spring-mass system. Each mass or element in this structure is represented by a one-dimensional model and is connected to its two neighboring elements in one dimension. Higher order FEM models can be obtained by properly interconnecting such one-dimensional FEM models.

Consider a mass-spring system with N identical discrete masses, each with mass M, connected together through $N-1$ identical springs, each with spring constant k. In addition, light viscous damping will be modeled independently for each of the $N-1$ masses as a dashpot with damping coefficient β between each mass and the reference frame. Assume that the mass at one end of the system is free and the mass at the other end is attached to a rigid point through an additional identical spring and dashpot. The inputs to the system are time-dependent external forces F_i applied independently to the individual masses. The system outputs are the positions and velocities of each of the masses as functions of time. The following set of equations describes the motion of such a system:

$$M\ddot{x_1} = -k(x_1) + k(x_2 - x_1) - \beta\dot{x}_1 + F_1 \tag{3.1}$$

$$M\ddot{x_i} = -k(x_i - x_{i-1}) + k(x_{i+1} - x_i) - \beta\dot{x}_i + F_i \qquad 2 \leq i < N \tag{3.2}$$

$$M\ddot{x_N} = -k(x_N - x_{N-1}) - \beta\dot{x}_N + F_N \tag{3.3}$$

where x_i is the displacement of the i^{th} mass from its nominal rest position. Note that these equations illustrate the repetitive structure mentioned previously about FEM models of flexible structures. These three types of equations are all that are necessary to emulate the entire system. As we have pointed out previously, it is often assumed that each of the elements in a FEM have identical inertia and stiffness properties.

In order to design the mass-spring circuit, one form of the following equation must be computed for each element:

$$\ddot{x}_n = -\frac{k}{M}(\alpha_1 x_{n-1} + \alpha_2 x_n + \alpha_3 x_{n+1}) - \frac{\beta}{M}\dot{x}_n + \Gamma F \tag{3.4}$$

where k is the spring constant, M is the mass of the suspended mass, β is the viscous damping coefficient, and x_n and $\dot{x}_n$ are the position and velocity of the n^{th} mass, respectively.

Equation (3.4) is general enough to include all three forms of the mass-spring FEM equations, (3.1) - (3.3). The resonant frequency ω_0 and the quality factor $Q = 1/2\zeta$ related to the damping of the free hanging mass taken as a single element are given by:

$$\omega_0 = \sqrt{\frac{k}{M}} \qquad Q = \frac{\sqrt{kM}}{\beta}. \tag{3.5}$$

A block diagram of the circuit representing an element with dynamics governed by (3.4) is shown in Figure 3.1. The circuit for the n^{th} element has input voltages representing the

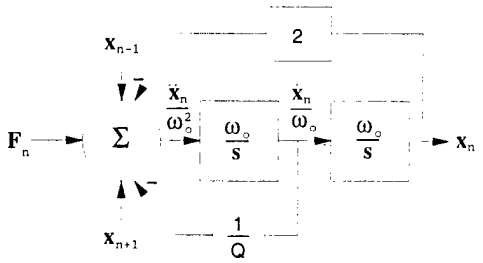

Figure 3.1: Block Diagram of the Mass-Spring Circuit

external force F_n applied to the element and the displacements x_{n-1} and x_{n+1} of each adjacent element. The output voltages from each circuit represent x_n and $\dot{x}_n$–the displacement and velocity of the element, respectively.

Thus, the circuit elements can be interconnected just as the actual mechanical elements would be interconnected as shown in Figure 3.2. External forces may be emulated by applying the appropriate voltage to each element via the available F_i inputs. These inputs correspond to the externally applied control inputs u in (2.2) and (2.3). Note that circuits may be designed with strings of these elements already connected on the integrated circuit chip. This would reduce the number of external connections required to produce an interconnected model.

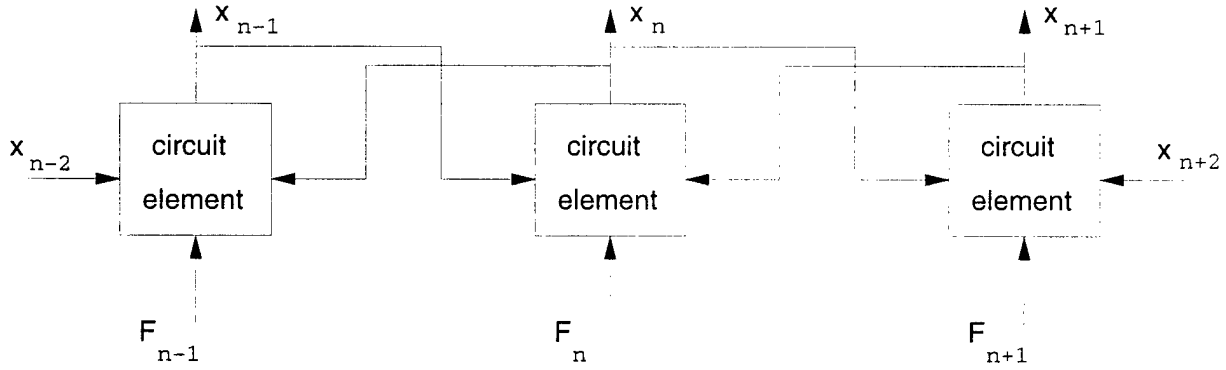

Figure 3.2: Interconnection of Circuit Elements

As more masses are added the system gains additional resonant modes. Table 3.1 shows how the modes change as masses are added for up to a 4 mass system.

It is useful for modeling physical systems that ω_0 be a low frequency. For example, an automobile suspension or flexible beam may have modes in the 10Hz or lower range. It is therefore an important goal to show that analog computation can work at low frequencies. For this reason the resonant mode was set at 100Hz and made tunable to achieve frequencies as low as 10Hz.

An important observation is that the integrator characteristic frequency ω_0 is used to set the

Table 3.1: Resonant Modes for Mass-Spring System

# Masses	Mode 1	Mode 2	Mode 3	Mode 4
1	ω_0			
2	$0.62\omega_0$	$1.62\omega_0$		
3	$0.45\omega_0$	$1.24\omega_0$	$1.80\omega_0$	
4	$0.35\omega_0$	$1.00\omega_0$	$1.53\omega_0$	$1.88\omega_0$

resonant frequency of the element. The characteristic frequency of an active RC integrator is given by $\omega_0 = \frac{1}{\tau}$ where $\tau = RC$ is the integrator time constant. It is therefore necessary to have very slow integrators on a VLSI chip, or in other words large RC time constants, a requirement which is directly opposed with the goal of miniaturization.

4. VLSI CIRCUIT DESIGN

The available technology which has been used is a two micron N-well double poly Orbit analog process. The circuit has been fabricated on a tiny chip which contains about $3.25mm^2$ of area. The supply rails have been set to $\pm 5V$.

4.1 Capacitance

In order to obtain fixed integrator time constants the integrator capacitors must be highly linear. The most linear capacitor available in this process is a double poly parallel plate capacitor. Unfortunately the unit area capacitance of a double poly capacitor is relatively small ($.47fF/\mu^2$). Therefore the largest practical capacitor size available is limited to about 30pF. This means that in order to obtain large RC time constants the resistance values will have to be extremely large.

4.2 Resistance

Given the goal of 100Hz characteristic frequency and capacitors limited to 30pF, the minimum resistance value will be approximately $50M\Omega$. Table 4.1 gives a list of maximum resistances for 5% of a tiny chip die area and also resistance per unit area for the various passive layers. It is clearly not feasible to use passive resistors to set the integrator frequency at 100Hz. The best alternative is to use active resistors.

In order to allow a greater variation in tuning without significant reduction of the input range, the double MOSFET method [6, 7, 8] is used. The double MOSFET method is a technique whereby a pair of matched resistors is replaced by four transistors[8]. The

Table 4.1: Comparison of Resistor Sizes

Resistor Layer	Maximum Resistance	Resistance/ Unit Area
Polysilicon	608 K	3.75 $\frac{\Omega}{\mu^2}$
N+ Active	540 K	3.33 $\frac{\Omega}{\mu^2}$
P+ Active	1.08 M	6.67 $\frac{\Omega}{\mu^2}$
N Well	16.3 M	101 $\frac{\Omega}{\mu^2}$
Active PMOS	158 M	975 $\frac{\Omega}{\mu^2}$

double MOSFET method requires that both resistors to be replaced must have a common voltage (V) on one node that is not electrically connected. Figure 4.1 shows how the double MOSFET method replaces a pair of resistors.

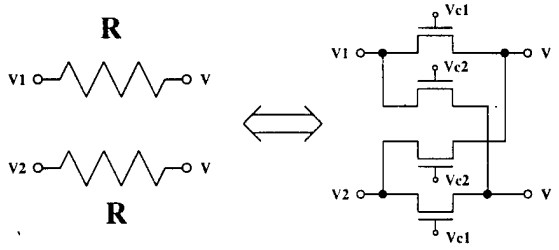

Figure 4.1: Double MOSFET Method to Replace Resistors

The equation for the voltage controlled equivalent resistance in this circuit is easily derived and given by:

$$R = \frac{L}{\mu C_{ox} W (V_{C1} - V_{C2})} \tag{4.1}$$

This equation is now independent of the input voltage to the resistor. It must be noted however that the MOS transistors must operate in the triode region, and thus:

$$V_1, V_2 \leq \min[V_{C1} - V_T, V_{C2} - V_T] \tag{4.2}$$

The main advantage of using the double MOSFET circuit in a fully balanced topology is that the tuning range is dramatically increased. Where a single MOSFET resistance is proportional to $1/(V_{GS} - V_T)$, the double MOSFET resistance is proportional to $1/(V_{C1} - V_{C2})$. This allows a minimum tuning range of a factor of 5 by allowing $\Delta V_C = (V_{C1} - V_{C2})$ to vary from $1V$ to $0.2V$.

4.3 Integrator Topology

The integrators used in the mass-spring circuit were implemented as shown in Figure 4.2. In order to reduce the distortion caused by MOS resistors a fully balanced folded cascode single-pole opamp is used. The implementation of an active MOSFET-C continuous-time filter requires the use of a fully balanced opamp[9, 10, 11, 12, 13, 14, 15]. A list of simulated performance specifications for the opamp is given in Table 4.2. The transfer function for the ideal integrator is given by:

$$\frac{V_{out}(s)}{V_{in}(s)} = \frac{\omega_0}{s} = \frac{1}{sRC} \tag{4.3}$$

Table 4.2: Folded Cascode Simulated Performance Specifications

Specification	Symbol	Value
Open Loop Gain	A_v	$70dB$
Unity Gain Bandwidth	F_t	$1.5MHz$
Phase Margin @ 150pF, 20K	PM	60°
Slew Rate @ 150pF, 20K	SR	$0.91V/\mu s$
Delay Time	t_d	$2.5\mu s$
Max. Common Mode Input	CMR_+	$3.3V$
Min. Common Mode Input	CMR_-	$-5.0V$
Maximum Output Voltage	V_{outMAX}	$3.3V$
Minimum Output Voltage	V_{outMIN}	-2.9
Maximum Load Capacitance	C_L	$150pF$
Minimum Resistive Load	R_L	$20K$
Static Power Dissipation	P_S	$15mW$
CM Feedback Loop Gain	A_{CMF}	$62dB$
CM Feedback Phase Margin	PM_{CMF}	70°
Positive Supply Voltage	V_{DD}	5V
Positive Supply Voltage	V_{SS}	-5V

The transistors used in the active resistors circuit for the integrator time constant were PMOS with a length of 2400μ and a width of 5μ. The equivalent resistance with typical process parameters and ΔV_C for the integrators set to $0.5V$ was $54M\Omega$. The capacitors were designed for 30pF, yielding an RC time constant of $1.62mS$, a characteristic frequency ω_0 of 98Hz.

4.4 Chip Layout

A full layout functional schematic of the chip is given in Figure 4.3. The integrator and weighted summer sections combine to form the transistor level implementation of the mass-spring circuit. The rest of the circuits on the chip are dedicated test structures. The required inputs sources are V_{DD}, V_{SS}, and I_{ref}, a reference current for the opamp. The opamp also requires bias voltages V_{B2} and V_{B3}. The tuning voltages are set by applying

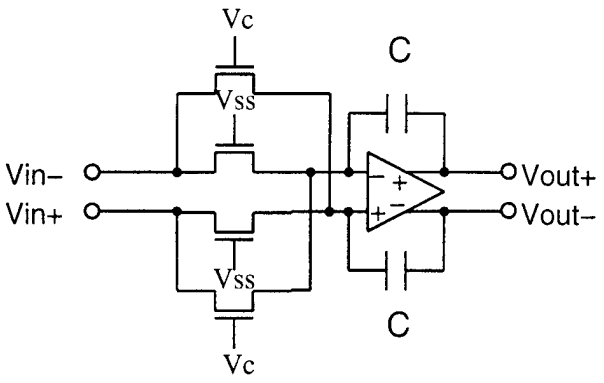

Figure 4.2: Integrator Topology

external voltages to V_C and V_Q. The mass-spring circuit has three external unity gain inputs to the weighted summer. These inputs are $V_{in1}+$, $V_{in1}-$, $V_{in2}+$, $V_{in2}-$, $F+$ and $F-$. Outputs are available for the position, velocity, and acceleration of each mass in the mass-spring system.

5. CHIP TEST SETUP AND RESULTS

5.1 Test Setup

The mass-spring circuit is designed to simulate the differential equation for one element of a vibrating mass-spring system. By properly interconnecting the circuits, systems of vibrating masses and springs are modeled. A MOSIS fabrication request provides 4 chips and therefore up to four vibrating masses can be simulated. The circuit allows for two external tuning voltages. The voltages are used to tune the vibration frequency $\omega_o = \sqrt{k/M}$ and the damping ratio $\zeta = \frac{1}{2Q}$. The circuit has been characterized by both a transfer function from the force on the free hanging mass to the velocity of the free hanging mass and by an impulse response from the free hanging mass to its velocity output. The following sections will demonstrate the performance of the mass-spring circuit.

5.2 Frequency Response

The primary characterization of the mass-spring system is the transfer function from the force input on the free mass to the velocity of that free mass. At a constant force (DC) the

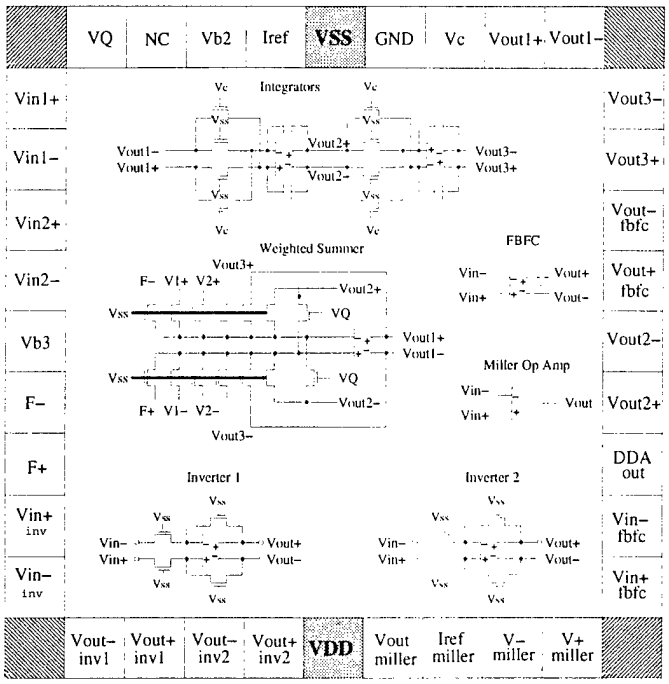

Figure 4.3: Functional Schematic for the Mass-Spring Chip

springs stretch a constant amount until the forces are equalized and then remain motionless. This corresponds to a zero at DC for the velocity and acceleration outputs.

The DC gain of the transfer function is scaled internally by the resistor weights of the weighted summer force input. Because the weighted summer is based on resistance ratios, there is also an external scaling available through external resistors. The transfer function can be attenuated to arbitrary values by using external resistances in series. The transfer function will be scaled by the ratio of $\frac{R}{R+R_{ext}}$ where R is the internal resistance from the weighted summer summer and R_{ext} is the external resistance added in series.

The transfer functions of the chip circuits have been measured with an HP3585B spectrum analyzer and plotted for one and four mass systems. The system is tuned to have resonant frequency of 100Hz for a single-mode one-element system. Transfer functions have been generated for one-element through four-element systems. The circuit transfer functions (dashed line) are plotted against the theoretical model transfer function (solid line). The plots are given in Figure 5.1 and Figure 5.2. The results show that the analog circuit model compares favorably with the mathematical model.

5.3 Impulse Response

The time domain equivalent of the transfer function is the impulse response. The impulse response is physically equivalent to an infinitely short unit energy hammer tap to the free

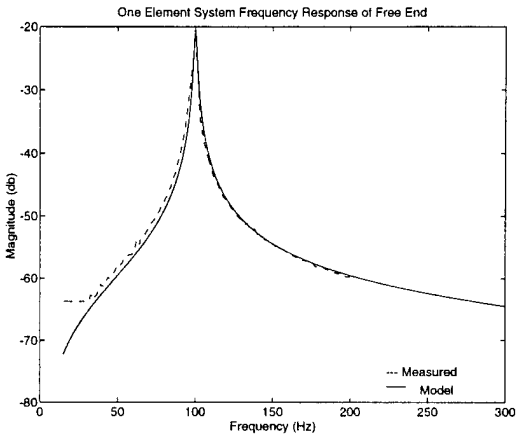

Figure 5.1: Single Mass System Frequency Response

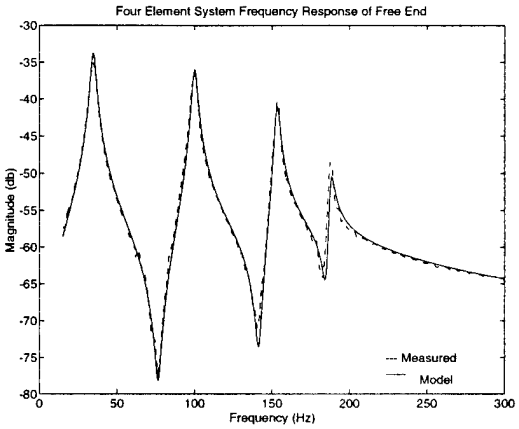

Figure 5.2: Four Mass System Frequency Response

mass. The impulse response is approximated by exciting the system with very fast impulse force generated by a function generator. The measured impulse response is shown in Figure 5.3. The FFT of the impulse response should be identical to the transfer function or frequency response. The FFT of the measured impulse response is shown in Figure 5.4 and is plotted against the measured frequency response. The two curves compare very favorably. One obvious difference is the high noise floor of the FFT due to quantization noise.

5.4 Tuning the Resonant Modes

The mass-spring circuit allows for tuning the center frequency via an external voltage. The frequency can actually be tuned over quite a large range of frequencies, at least a factor of 10 from maximum to minimum. Figure 5.5 shows the measured frequency response for a one spring system tuned for different resonant frequencies. The tuning range varies from

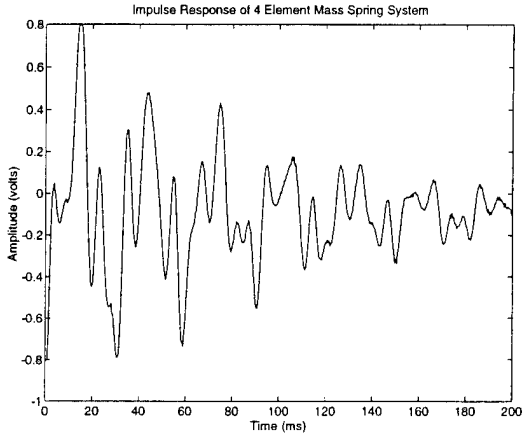

Figure 5.3: Four Mass System Impulse Response

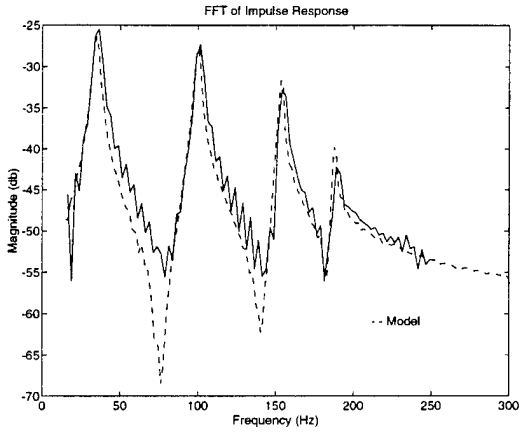

Figure 5.4: FFT of Four Mass System Impulse Response

about 10 to 200 Hz.

5.5 Tuning the Damping Ratio

The damping ratio can be also be tuned via an external voltage. Figure 5.6 shows the effect of tuning the damping on the measured frequency response of a one mass system. The Q can be tuned from about 10 to 100 which is close to a ζ from 0.005 to about 0.05 The curves clearly show that the damping in the model can be controlled from nearly undamped to significantly damped.

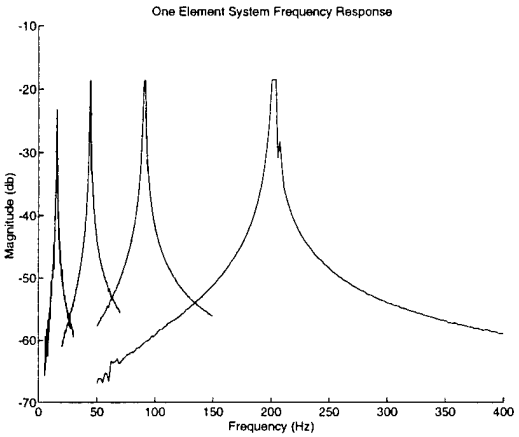

Figure 5.5: Effect of Tuning the Center Frequency

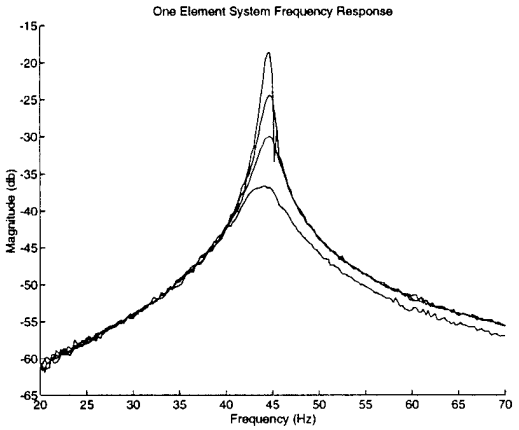

Figure 5.6: Effect of Tuning the Damping Ratio

6. MODEL-BASED CONTROL OF FLEXIBLE STRUCTURES USING CIRCUIT ANALOGIES

As mentioned previously, the primary motivation for developing these VLSI circuit models of flexible structures if for inclusion in model-based controller designs. Model-based control includes such methods as observer-based control, adaptive control, and several robust control schemes. A general system diagram of a model-based control system is shown in Figure 6.1. In this diagram, y is the vector of measured outputs, u is the vector of control inputs which are applied to the plant, and r represents the vector of reference signals. Regardless of the type of control scheme used, the model-based controller receives the measured outputs and applied inputs to compare with its internal model of the plant. Based on these comparisons, it determines an appropriate control signal.

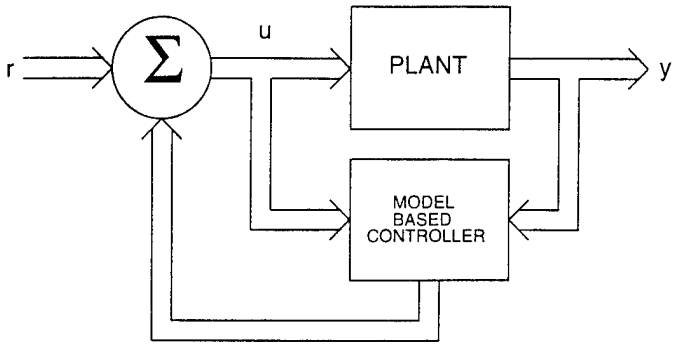

Figure 6.1: Model-based control system

In any of these control methods, cost and size are key advantages of using VLSI circuit models of flexible structures. A model may be easily mounted to the structure or substructure to be controlled and used either as an observer or as part of an integrated controller. Because this model is analog, a microprocessor may not be necessary for control.

As discussed previously, the dynamical equations of a structure are equivalent to the dynamical equations of the analogous RLC circuit. The state equations for a nondegenerate RLC circuit (no capacitance-voltage source loops and no inductance-current source cut sets) without controlled (dependent) sources can be written as

$$L\frac{di_L}{dt} = Ri_L + A_C v_C + B_E E(t) \tag{6.1}$$

$$C\frac{dv_C}{dt} = A_L i_L + Gv_C + B_I I(t) \tag{6.2}$$

where the following are defined:

i_L	vector of inductor currents
v_C	vector of capacitor voltages
$E(t)$	vector of independent voltage sources
$I(t)$	vector of independent current sources
L	inductance matrix
C	capacitance matrix
R	matrix of resistances in writing loop (voltage) equations (row j shows resistances in the same loop as L_{jj})
A_C	matrix showing capacitor voltages in loop (entries ± 1 or 0)
B_E	matrix showing voltage sources in loop (entries ± 1 or 0)
G	matrix of inverse resistances in writing cut set (current) equations
A_L	matrix showing inductor currents in cut set (entries ± 1 or 0)
B_I	matrix showing current sources in cut set (entries ± 1 or 0)

Note that these state equations may be rewritten in the form

$$\dot{x} = Ax + Bu \tag{6.3}$$

where the state $x = [i_L^T \; v_C^T]^T \in \mathbb{R}^n$ is equivalent to the forces and velocities in the actual physical structure, $u = [E^T \; I^T]^T$ is equivalent to the external velocity and force inputs,

and

$$A = \begin{bmatrix} L^{-1}R & L^{-1}A_c \\ C^{-1}A_L & -C^{-1}G \end{bmatrix} \qquad B = \begin{bmatrix} L^{-1}B_E \\ C^{-1}B_I \end{bmatrix}. \tag{6.4}$$

6.1 Observer Design

Observer design is one interesting application of circuit representations of flexible structures. The observer may be easily mounted to the structure or substructure to be controlled. This observer can be implemented with an analog VLSI circuit model of the original system.

The observer for the structure is equivalent to the observer for the analogous RLC circuit. Consider the case with some voltage (velocity) measurements. Thus,

$$y = \begin{bmatrix} 0 & H \end{bmatrix} \begin{bmatrix} i_L \\ v_C \end{bmatrix} \tag{6.5}$$

where it is assumed that H has full row rank and that $\{A, [0\ H]\}$ is observable. An observer can be designed using the circuit model of the structure such that the error between the observed states $\hat{x} = [\hat{i}_L^T\ \hat{v}_C^T]^T \in \mathbb{R}^n$ and the true states which are the forces and velocities of the structure can be driven to zero with error dynamics specified by the selection of matrices F_1 and F_2 resulting in the following equations:

$$L\frac{d\hat{i}_L}{dt} = R\hat{i}_L + A_C\hat{v}_C - LF_1H\hat{v}_C + LF_1y + B_EE(t) \tag{6.6}$$

$$C\frac{d\hat{v}_C}{dt} = A_L\hat{i}_L + G\hat{v}_C - CF_2H\hat{v}_C + CF_2y + B_II(t) \tag{6.7}$$

These equations imply that controlled (dependent) voltage sources must be added to the inductive element nodes with gains represented by F_1 and that controlled (dependent) current sources must be added to the capacitive element nodes with gains represented by F_2. Thus, an observer for a mechanical substructure may be created using the VLSI circuit model of the substructure driven by outputs of the system with the addition of dependent sources either external or internal to the VLSI chip. The resulting observed states will approach the true states asymptotically and may then be employed in state feedback control design [16].

6.2 Sensitivity Modeling and Adaptive Control

A second specific application of the available analog VLSI circuit is to generate the so-called sensitivity functions of the states of a structure with respect to a vector α of unknown parameters of interest. It is assumed that the physical system matrices such as mass, stiffness, and damping which are represented by the electrical equivalents C, L, R, and G are known functions of an unknown parameter vector $\alpha \in \mathbb{R}^p$ such that the system

behavior is directly effected by variations of α. In fact, the physical system matrices are, indeed, functions of such unknown parameters as Young's modulus, the shear modulus, and the density of a material. These parameters are generally *approximated* experimentally, but are not known exactly.

It is known that the sensitivity functions can be generated from a sensitivity model which is governed by the same dynamics as the original system model and is driven by the system outputs [17, 18]. For the open-loop case where the system input u is not a function of α, the sensitivity model for the system represented by (6.1) and (6.2) is given by

$$L\frac{d}{dt}\frac{\partial i_L}{\partial \alpha_i} = R\frac{\partial i_L}{\partial \alpha_i} + A_C\frac{\partial v_C}{\partial \alpha_i} + \frac{\partial R}{\partial \alpha_i}i_L - \frac{\partial L}{\partial \alpha_i}\frac{di_L}{dt} \qquad i = 1,\ldots,p \tag{6.8}$$

$$C\frac{d}{dt}\frac{\partial v_C}{\partial \alpha_i} = A_L\frac{\partial i_L}{\partial \alpha_i} + G\frac{\partial v_C}{\partial \alpha_i} + \frac{\partial G}{\partial \alpha_i}v_C - \frac{\partial C}{\partial \alpha_i}\frac{dv_C}{dt}. \tag{6.9}$$

Thus, as with the observer, the sensitivity functions $\partial x/\partial \alpha_i$ can be generated with the VLSI circuit model by adding dependent sources either external or internal to the VLSI chip. Note that the dynamics associated with this sensitivity model are mathematically similar to the original system model. These equations may be rewritten in a form similar to (6.3) from Section 6.1

$$\frac{d}{dt}\frac{\partial x}{\partial \alpha_i} = A\frac{\partial x}{\partial \alpha_i} + B\frac{\partial u}{\partial \alpha_i} + \frac{\partial A}{\partial \alpha_i}x + \frac{\partial B}{\partial \alpha_i}u. \tag{6.10}$$

For simplicity, the notation of (6.3) and (6.4) will be adopted for the remainder of this chapter.

The resulting sensitivity functions may then be used in parameter identification and indirect adaptive control algorithms often referred to as gradient descent or sensitivity methods [17, 18, 19, 20]. In the controller design, a control structure is assumed and a design method is chosen such that the controller parameters depend on the system parameters by some known relationship. Because the system parameters depend on the unknown parameters α, the controller parameters also depend on α based on a known relationship. The basic philosophy behind indirect adaptive control is to obtain an estimate $\hat{\alpha}$ of the actual parameter vector α in real-time and to use $\hat{\alpha}$ to determine the controller parameters as if the estimates were the true parameters.

In the adaptive control scheme we propose, several VLSI circuit models of the system using the estimated parameters $\hat{\alpha} \in \mathbb{R}^p$ will be used within the controller structure. As has been shown in the previous chapter, the circuit parameters are tunable and will be updated continuously with new parameter estimates. The states of one of the models will be denoted by $\tilde{x} = x(\hat{\alpha})$ and will be used as an internal model of the physical system being controlled. Thus,

$$\dot{\tilde{x}} = \tilde{A}\tilde{x} + \tilde{B}u \tag{6.11}$$

where $\tilde{A}$ and $\tilde{B}$ are equivalent to A and B in (6.4) evaluated using the *estimated* parameters rather than the *true* parameters. Furthermore, for each estimated parameter $\hat{\alpha}_i$, a separate VLSI circuit sensitivity model similar to the model described in (6.10) will be used.

The gradient descent or sensitivity methods of identifying α seek to minimize the error $e = x - \tilde{x}$ (or some cost functional of e) between the the actual system state x and the state $\tilde{x}$ of the internal model. It is assumed that the actual state x is available for measurement and that $\tilde{x}(0) = x(0)$ is chosen as the initial conditions of the internal model. This eliminates any errors between x and $\tilde{x}$ due to differences in the initial conditions such that all of the state errors are assumed to be due to the error between α and $\hat{\alpha}$.

Consider the positive definite cost functional and Lyapunov function candidate

$$J = \frac{1}{2} e^T e. \tag{6.12}$$

From Lyapunov stability theory, it is well known that if the time derivative of J

$$\frac{dJ}{dt} = \frac{\partial J}{\partial \hat{\alpha}} \frac{d\hat{\alpha}}{dt} = \frac{\partial J}{\partial e} \frac{\partial e}{\partial \hat{\alpha}} \frac{d\hat{\alpha}}{dt} \tag{6.13}$$

could be made negative definite, then the error will approach zero asymptotically. Although, in general, it is not possible to guarantee that dJ/dt is negative definite, it is possible to ensure that dJ/dt be negative semi-definite by varying $\hat{\alpha}$ along the negative of the gradient of J as

$$\frac{d\hat{\alpha}_i}{dt} = -\gamma_i \frac{\partial J}{\partial \hat{\alpha}_i}^T = -\gamma_i \frac{\partial e}{\partial \hat{\alpha}_i}^T \frac{\partial J}{\partial e}^T = -\gamma_i \left(\frac{\partial e}{\partial \hat{\alpha}_i} \right)^T e \qquad i = 1, \ldots, p \tag{6.14}$$

where the γ_i are positive constants which control the rate of convergence of the parameter estimates to the true values. These constants are often referred to as the adaptation gains. With the above choice of $d\hat{\alpha}/dt$, the derivative of the cost functional becomes

$$\frac{dJ}{dt} = -e^T \left(\sum_{i=1}^{p} \gamma_i \frac{\partial e}{\partial \hat{\alpha}_i} \frac{\partial e}{\partial \hat{\alpha}_i}^T \right) e \tag{6.15}$$

which is obviously negative semi-definite.

To use the parameter estimation scheme described by (6.14), $\partial e / \partial \hat{\alpha}_i$ must be evaluated

$$\frac{\partial e}{\partial \hat{\alpha}_i} = \frac{\partial x}{\partial \hat{\alpha}_i} - \frac{\partial \tilde{x}}{\partial \hat{\alpha}_i}. \tag{6.16}$$

The $\partial \tilde{x} / \partial \hat{\alpha}_i$ term is obtained from the sensitivity model

$$\frac{d}{dt} \frac{\partial \tilde{x}}{\partial \hat{\alpha}_i} = \tilde{A} \frac{\partial \tilde{x}}{\partial \hat{\alpha}_i} + \tilde{B} \frac{\partial u}{\partial \hat{\alpha}_i} + \frac{\partial \tilde{A}}{\partial \hat{\alpha}_i} \tilde{x} + \frac{\partial \tilde{B}}{\partial \hat{\alpha}_i} u. \tag{6.17}$$

Similarly, noting that the system matrices A and B of the actual structure are not functions of $\hat{\alpha}$, the $\partial x/\partial \hat{\alpha}_i$ term is obtained from the sensitivity model

$$\frac{d}{dt}\frac{\partial x}{\partial \hat{\alpha}_i} = A\frac{\partial x}{\partial \hat{\alpha}_i} + B\frac{\partial u}{\partial \hat{\alpha}_i}. \tag{6.18}$$

As the true matrices A and B are unknown, this sensitivity model will be evaluated using $\tilde{A}$ and $\tilde{B}$ which are based on the estimated parameters [17, 18].

For open-loop parameter identification, the input u is not a function of $\hat{\alpha}$; thus, the $\partial x/\partial \hat{\alpha}_i$ terms are zero. However, for closed-loop parameter identification, $u = r + Kx$ where r is a vector of independent reference signals and K is the feedback gain matrix whose parameters are functions of $\hat{\alpha}$. Thus, $\partial x/\partial \hat{\alpha}_i$ must be evaluated because $\partial u/\partial \hat{\alpha}_i$ is nonzero in general

$$\frac{\partial u}{\partial \hat{\alpha}_i} = \frac{\partial K}{\partial \hat{\alpha}_i}x + K\frac{\partial x}{\partial \hat{\alpha}_i}. \tag{6.19}$$

Substituting (6.19) into (6.17) and (6.18) and evaluating (6.16) yields

$$\frac{d}{dt}\frac{\partial e}{\partial \hat{\alpha}_i} = \tilde{A}\frac{\partial e}{\partial \hat{\alpha}_i} - \frac{\partial \tilde{A}}{\partial \hat{\alpha}_i}\tilde{x} - \frac{\partial \tilde{B}}{\partial \hat{\alpha}_i}u. \tag{6.20}$$

Thus, the error sensitivity functions are obtained from the analog VLSI circuit models and used in the gradient descent parameter identification scheme to obtain parameter estimates $\hat{\alpha}$. These estimates are then used to update the internal model, the sensitivity models, and the controller parameters. A simple example is provided in the following section.

6.3 Adaptive Control of a Mass-Spring System

In this section, simulation results of the above adaptive control scheme for a single mass-spring element will be presented to illustrate the concept of vibration control using the developed VLSI circuits. Consider once again the mass-spring system model of Chapters 3 and 4 for a single finite element with mass M, stiffness k, and damping coefficient β. In this example, it will be assumed that the stiffness and damping coefficient are incorrectly estimated *a priori* as shown in Table 6.1. Thus, the uncertain parameter vector is $\alpha = [\beta\ k]^T$. The values in the table have been chosen to represent typical values of a single finite element for a structural model. It should be noted that in practice, a very large number of these elements could be integrated on a single chip to emulate the complete model of a larger, more complex substructure.

The equations of motion for the actual system can be written in the equivalent form of (6.1) and (6.2) using the circuit analogies presented in Table 2.2

$$\frac{1}{k}\frac{df_s}{dt} = v \tag{6.21}$$

$$M\frac{dv}{dt} = -f_s - \beta v + F \tag{6.22}$$

Table 6.1: Parameters for Mass-Spring Example

Parameter	Actual Value	Nominal Estimate
M, kg	0.01	0.01
k, N/m	100	90
β, $N{\cdot}s/m$	0.02	0.05

where $v = \dot{x}$ is the velocity of the mass, f_s is the force of the spring, and F is the externally applied force input which is available for control. These equations can be written in the state space form of (6.3) where $x = [f_s \;\; v]^T$, $u = F$, and

$$A = \begin{bmatrix} 0 & k \\ -\frac{1}{M} & -\frac{\beta}{M} \end{bmatrix} \qquad B = \begin{bmatrix} 0 \\ -\frac{1}{M} \end{bmatrix}. \tag{6.23}$$

The nominal model based on the estimated parameters

$$\frac{1}{\hat{k}}\frac{d\tilde{f}_s}{dt} = \tilde{v} \tag{6.24}$$

$$\hat{M}\frac{d\tilde{v}}{dt} = -\tilde{f}_s - \hat{\beta}\tilde{v} + F \tag{6.25}$$

can similarly be written in the form of (6.11) where $\tilde{x} = [\tilde{f}_s \;\; \tilde{v}]^T$ and

$$\tilde{A} = \begin{bmatrix} 0 & \hat{k} \\ -\frac{1}{\hat{M}} & -\frac{\hat{\beta}}{\hat{M}} \end{bmatrix} \qquad \tilde{B} = \begin{bmatrix} 0 \\ -\frac{1}{\hat{M}} \end{bmatrix}. \tag{6.26}$$

The error sensitivity models corresponding to each parameter are obtained from (6.20) and the parameter estimates are updated using the gradient descent method described by (6.14).

In typical flexible structure control designs, a common objective is to add significant damping to the flexible modes for the purpose of reducing vibrations. However, it is often the case that quick translational or slewing maneuvers may be necessary which often excite the flexible modes. A square wave has been used to emulate the rigid body position reference command r. The controller structure is assumed to be $u = r + Kx$ where the feedback gain matrix K can be designed using any of various state-space methods. For this simple second order example, the design objective shall merely be to place the poles such that the response will be relatively quick and have a significant increase in damping. To obtain a desired natural frequency of oscillation $\omega_d = 1500 rad/s$ and a desired damping ratio of $\zeta_d = 0.7$, the characteristic equation $s^2 + 2\zeta_d\omega_d s + \omega_d^2 = 0$ is set equal to the determinant of the closed-loop system matrix $\tilde{A} + \tilde{B}K$. Hence, the resulting gains are functions of the estimated parameters

$$K = [K_1 \;\; K_2] = \left[1 - \omega_d^2\frac{\hat{M}}{\hat{k}} \quad \hat{\beta} - 2\zeta_d\omega_d\hat{M}\right]. \tag{6.27}$$

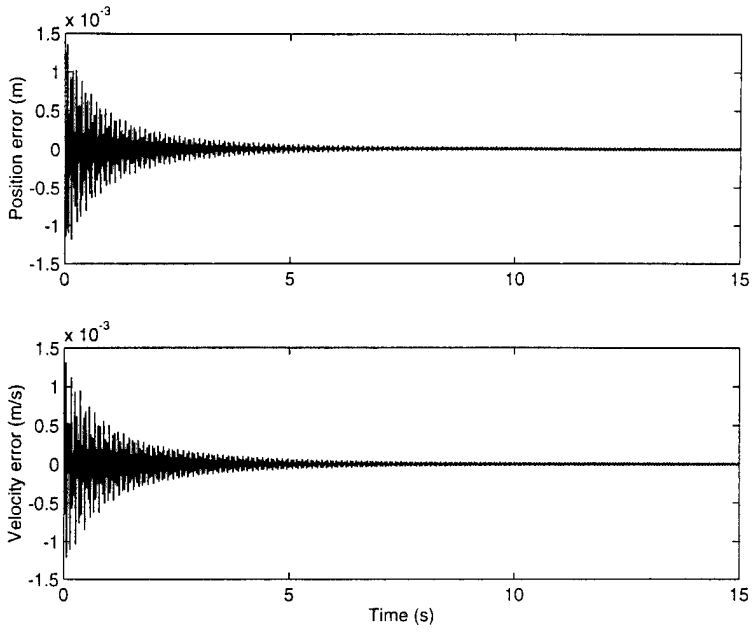

Figure 6.2: Error Between Actual System States and Internal Model States

As shown in Figure 6.2, the magnitudes of the errors between the actual system states and the internal model states approach zero asymptotically. Furthermore, the uncertain parameter estimates do converge to the actual parameter values as shown in Figure 6.3. The response shown in Figure 6.4 of the actual system to the square wave position reference command after adaptation illustrates the desired quick translational motion with very little oscillation. These results indicate that the developed adaptive control scheme which utilizes the developed analog VLSI circuit models performs well.

7. CONCLUSION

The AASERT support has allowed us to investigate integrated circuits for distributed control of flexible structures. This report has presented work concerning circuit implementations of finite element models of flexible structures and model-based control approaches in which these circuits are used.

An analog VLSI prototype has been developed and tested. A technique has been presented to implement low frequency finite element models with analog VLSI circuits. Four chips have been fabricated, each containing a single finite element of a mass-spring system. Results were presented for a four element mass-spring system, and proved to be very accurate in

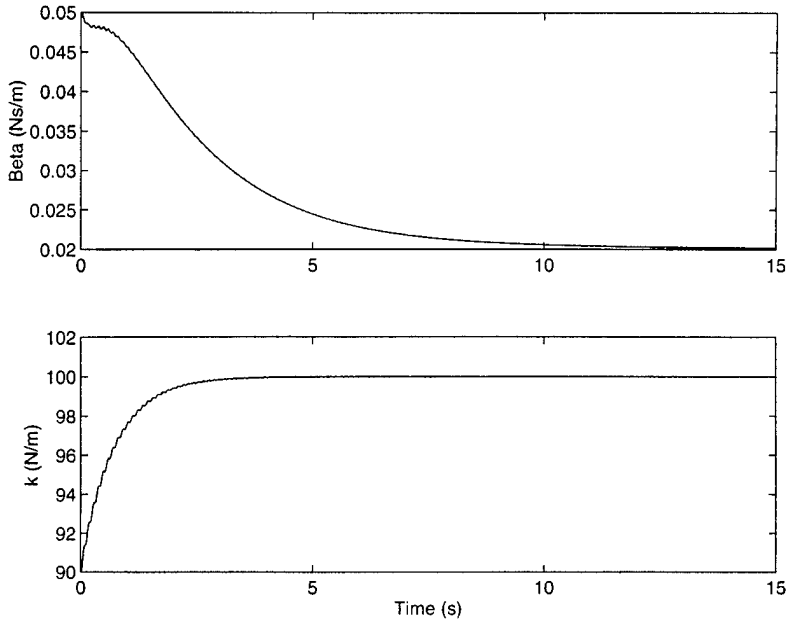

Figure 6.3: Convergence of Internal Model Parameters to Actual System Parameters

comparison to the theoretical model. The mass-spring system has also been extended in discrete form to a two-state flexible beam element with similar results. The number of elements and the number of states per element can be easily extended. The high precision of results is due in part to manual tuning of the integrator time constants, but future designs could incorporate automatic tuning schemes such as those presented in the adaptive control section of this report.

The success of these analog FEM models creates the possibility for low area, low cost model-based controllers for vibrating systems which may be integrated with the actuation and embedded into the structure or substructure. It has been shown how these VLSI circuit models could be employed in several model-based control schemes. Simulation results of an adaptive vibration controller of a simple mass-spring system using the developed VLSI models have also been presented.

REFERENCES

[1] Ü. Özgüner and L. Lenning, "The intelligence between sensing and actuation in smart structures," in *Proceedings of the ADPA/AIAA/ASME/SPIE Conference on Active Materials and Adaptive Structures*, pp. 825–830. The Institute of Physics, 1992.

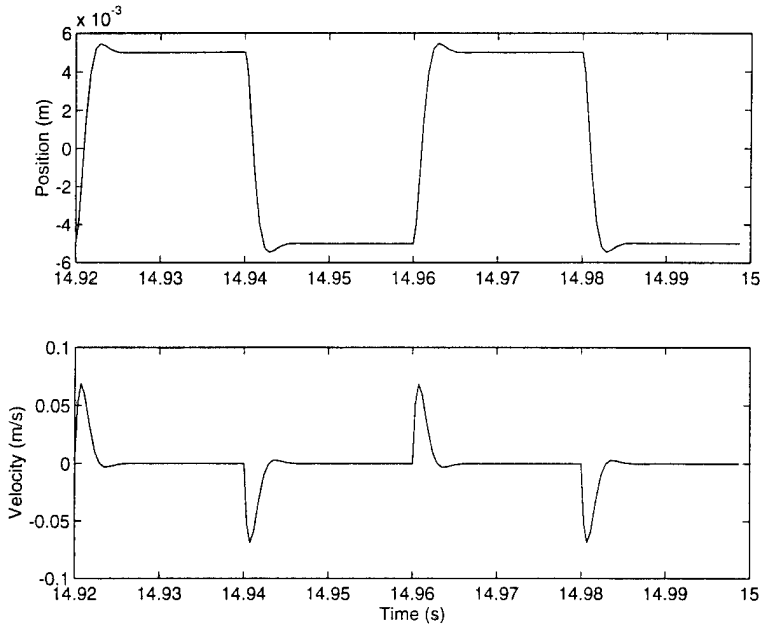

Figure 6.4: Actual System Response after Adaptation

[2] A. Shah, L. Lenning, S. Bibyk, and Ü. Özgüner, "Flexible beam modeling with analog VLSI circuits," in *Adaptive Structures and Composite Materials: Analysis and Application*, vol. AD-45/MD-54, pp. 261–265, ASME, 1994.

[3] A. Shah, L. Lenning, Ü. Özgüner, and S. Bibyk, "Analog VLSI circuit models for smart flexible structures," in *Smart Structures and Materials 1995: Mathematics and Control in Smart Structures* (V. V. Varadan, ed.), Proc. SPIE 2442, 1995.

[4] L. Meirovitch, *Elements of Vibration Analysis.* New York: McGraw-Hill, 1986.

[5] R. D. Cook, *Concepts and Applications of Finite Element Analysis.* New York: John Wiley & Sons, 1974.

[6] Z. Czarnul, "Modification of the Banu-Tsividis continuous-time integrator structure," *IEEE Transactions on Circuits and Systems*, vol. CAS - 33, pp. 714–716, July 1986.

[7] Y. Tsividis, M. Banu, and J. Khoury, "Continuous-time MOSFET-C filters in VLSI," *IEEE Journal of Solid-State Circuits*, vol. SC - 21, pp. 15–30, February 1986.

[8] M. Ismail, S. Smith, and R. Beale, "A new MOSFET-C universal filter structure for VLSI," *IEEE Journal of Solid-State Circuits*, vol. 23, pp. 183 – 194, February 1988.

[9] P. R. Gray and R. G. Meyer, *Analysis and Design of Analog Integrated Circuits.* New York: John Wiley and Sons, 3rd ed., 1993.

[10] P. E. Allen and D. R. Holberg, *CMOS Analog Circuit Design.* New York: Holt, Rinehart, and Winston, 1987.

[11] P. R. Gray and R. G. Meyer, "MOS operational amplifier design - a tutorial overview," *IEEE Journal of Solid-State Circuits*, vol. SC - 17, pp. 969 – 982, December 1982.

[12] C. Wu, P. Lu, C. Lee, and M. Tsai, "New fully differential HF CMOS op amps with efficient common mode feedback," in *Proceedings of the 1989 ISCAS*, pp. 2076 – 2079, 1989.

[13] P. VanPeteghem and J. Duque-Carrillo, "A general description of common mode feedback in fully differential amplifiers," in *Proceedings of the 1990 ISCAS*, pp. 3209 – 3212, 1990.

[14] M. Banu, J. M. Khoury, and Y. Tsividis, "Fully differential operational amplifiers with accurate output balancing," *IEEE Journal of Solid-State Circuits*, vol. 23, pp. 1410 – 1414, December 1988.

[15] S. Levy, P. Hurst, P. Ju, and C. Cole, "A single chip 5-V 2400-b/s modem," *IEEE Journal of Solid-State Circuits*, vol. 25, pp. 632 – 643, June 1990.

[16] C.-T. Chen, *Linear System Theory and Design.* New York: Holt, Rinehart and Winston, 1984.

[17] J. B. Cruz, *Feedback Systems*, vol. 14 of *Inter-University Electronics Series.* New York: McGraw-Hill, 1972.

[18] P. M. Frank, *Introduction to System Sensitivity Theory.* New York: Academic Press, 1978.

[19] K. S. Narendra and A. M. Annaswamy, *Stable Adaptive Systems.* Englewood Cliffs, New Jersey: Prentice-Hall, 1989.

[20] K. Åström and B. Wittenmark, *Adaptive Control.* Reading, Massachusetts: Addison-Wesley, 1989.